AIAA JOURNAL
Vol. 34, No. 10, October 1996

Local Buckling of Delaminated Composite Sandwich Plates

Chien-Chang Lin* and Shou-Hsiung Cheng†
National Chung-Hsing University, Taiwan 402, Republic of China
and
James Ting-Shun Wang‡
Georgia Institute of Technology, Atlanta, Georgia 30332

A two-dimensional model of the delaminated face sheet of sandwich plates for predicting local buckling using continuous analysis is presented. The analysis procedure can handle without difficulty sandwich plates having single or multiple embedded delaminations of various shapes and sizes at any locations. The continuous analysis treats the delamination between a face sheet and the core as a continuous system of a perfectly bonded laminate on the core but with an added fictitious force system to make interfacial tractions to vanish over the delaminated region. The method presented in the study is straightforward, simple, and accurate for determining the buckling load of delaminated sandwich plates. A number of numerical results accounting for the effects of transverse normal and shear stiffnesses of the core on the buckling load of sandwich plates having delaminations of various shapes and sizes at different locations are presented. The illustrative examples indicate that the present method is effective and useful for practical applications.

Nomenclature

A_{ij} = laminate extensional stiffness
A_{eff} = effective contact area of core per unit area of face plate
a, b = length and width of rectangular sandwich plate
a_d, b_d = length and width of rectangular delamination
c = thickness of core
D_{ij} = laminate bending stiffness
E_c = Young's modulus of core in the z direction
G_{xz}, G_{yz} = transverse shear moduli of the core
k_f = transverse normal resistance of core, $\equiv E_c \cdot A_{\text{eff}}/c$
$\bar{k}_f, \bar{s}_x, \bar{s}_y$ = nondimensional transverse normal and shear stiffnesses of core; $\bar{k}_f \equiv k_f b/E_2\pi$, $\bar{s}_x \equiv s_{fx}b/E_2\pi$, and $\bar{s}_y \equiv s_{fy}b/E_2\pi$
N = number of discrete points taken in the delaminated region
P_x = uniaxial buckling load in the x direction
$q(x, y)$ = distributed transverse force from the foundation
q_i = added transverse forces at discrete points in the delaminated region
$R(x, y)$ = y component of transverse shear stress from the core
R_i = added transverse shear force in y direction at ith discrete point in the delaminated region
r_d = radius of circular delamination
t = thickness of face sheet
u, v, w = displacements of face sheet
$V(x, y)$ = x component of transverse shear stress from the core
V_i = added transverse shear force in x direction at ith discrete point in the delaminated region

Introduction

DELAMINATION is one of the most common flaws in composite structures. Delaminations may occur as a result of various reasons such as manufacturing imperfections, impact of foreign objects, or high stress concentrations in the area of geometric or material discontinuities. Delaminations reduce the stiffness of the structure and make it easier to buckle under compressive load.

Sandwich plates consisting of orthotropic or anisotropic face sheets separated by core material have widespread applications because they are capable of providing lightweight construction. Needless to say, new materials such as nonmetallic honeycombs and plastic foams are often used as core materials, and the fiber-reinforced composite laminates are increasingly used for face sheets. For composite sandwiches, the interface between the face and core may be weaker than those in layered composite laminates or core materials. Generally speaking, delaminated composite sandwiches are referred to as sandwiches having interface cracks between a face sheet and the core. This study focuses on the sandwich plates having single or multiple embedded delaminations.

Since Chai et al.[1] established the one-dimensional model for the buckling analysis of beam plates with delaminations, a number of investigations[2–8] concerned with this subject have been presented. Studies on two-dimensional modeling for buckling analysis of elliptic delamination under compression can be found in Refs. 9–14. Although there are studies dealing with buckling of composite sandwich beams, such as Refs. 15–17, most earlier investigations do not involve delamination. Kardomateas[18] extended the work by Kardomateas and Schmueser[6] for the case of a beam plate on an elastic foundation. Somer et al.[19] developed a theoretical model based on the earlier work of Chai et al.[1] to study the local buckling of a delaminated sandwich beam. Frostig[20] investigated the delamination behavior at one of the skin–core interfaces in a beam. Hwu and Hu[21] presented a one-dimensional mathematical model similar to that by Chai et al.[1] for analyzing the overall buckling of delaminated sandwich beams. Based on the continuous analysis method of Wang,[22] Cheng et al.[23] presented a one-dimensional analytical model for the local buckling of a delaminated sandwich beam. Wang and Huang[24] employed continuous analysis to evaluate the strain energy release rate of delaminated composite plates. However, no analytical work has been found by the author in open literature concerning problems of sandwich plates having multiple delaminations with various shapes, sizes, and locations.

The objective of this study is to formulate an analytically tractable two-dimensional model accounting for the normal as well as tangential resistance of the core to the face sheets for the title problem on one hand and to demonstrate the applicability of the analytical procedure of the continuous analysis for analyzing the discontinuous sandwich structures with delaminations on the other. It appears to be too difficult if not impossible to analyze such structures with delaminations of arbitrary numbers, shapes, and locations. Although other numerical procedures such as the finite difference, finite element, or boundary element methods are powerful tools, which are capable of handing complex problems such as the present one, they are suited

Received Nov. 28, 1995; revision received May 1, 1996; accepted for publication June 25, 1996.

*Professor, Department of Applied Mathematics. Associate Fellow AIAA.
†Graduate Assistant, Department of Applied Mathematics.
‡Professor Emeritus, School of Civil and Environmental Engineering.

for specific problems and become cumbersome and not economical for exploratory studies as one must generate meshes for each individual case separately in general. Although the accuracy of these numerical procedures depend on the model of the elements used, it is generally difficult to assess the errors involved; the continuous analysis procedure provides the solutions of the governing differential equations that should accurately describe the behavior of the entire structure. Since the continuous analysis procedure can be used for delaminated structures as long as the exact solutions for the corresponding structure without delamination can be obtained, we have considered rectangular plates for which solutions are represented by Fourier series; solutions presented in this study are anticipated to converge to exact solutions. Since the continuous analysis method has no limitation on its applicability to disbonded structures, and the procedure is simple to follow and effective, it is more suitable for the present problem than other numerical procedures, including the finite element analysis. Consequently, the continuous analysis method is used in the study.

Formulation

The local buckling of one of the face sheets made of fiber-reinforced composites having a multiple number of disbonds from the core is considered. The usual assumptions that the sheets are much thinner than the core, that only transverse normal and shear resistance to the face sheets are provided by the core, and that there is no coupling of transverse normal and shear resistance are considered. Consequently, face sheets take all the in-plane loading. These basic assumptions have been commonly used as may be traced back in the early work of Heath[25] on sandwich structures. If the shear resistance of the core is neglected, the problem reduces to a plate on a Winkler foundation, and only transverse displacement as a result of bending of the plate is involved. Since the normal as well as shear stiffnesses of the core are accounted for in the present study, the analysis becomes much more involved as the in-plane forces and deformation are coupled with the bending and transverse displacement of the face sheet. Following the same idea used in Ref. 23, the modified continuous model, based on the commonly accepted Kirchhoffean plate theory, for this case is shown in Fig. 1. We consider that any ith subdivision in the debonded region is the same as the element in the perfectly bonded region on an elastic foundation of the core but with unknown fictitious normal and shear forces q_i, V_i, and R_i added in each subdivision so that the net traction at the interface at every subdivision vanishes during buckling. According to the aforementioned model for the continuous analysis procedure, we divide the debonded region into N subdivisions and require that the conditions

$$\iint_{\Delta A_i} q(x, y)\,dx\,dy = q_i, \qquad \iint_{\Delta A_i} V(x, y)\,dx\,dy = V_i$$

and

$$\iint_{\Delta A_i} R(x, y)\,dx\,dy = R_i$$

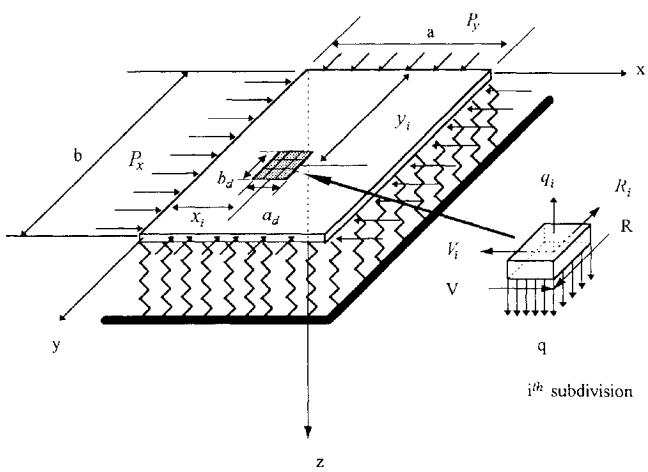

Fig. 1 Model of sandwich face plates for continuous analysis.

be satisfied at each subdivision in the delaminated region, which leads to $3N$ equations for N sets of three unknown fictitious forces and the buckling load parameters.

The equilibrium equations governing the buckled state of the face sheet are as follows:

$$\frac{\partial N_x}{\partial x} + \frac{\partial N_{xy}}{\partial y} + V - \sum_{i=1}^{N} V_i \delta(x - x_i)\delta(y - y_i) = 0 \tag{1a}$$

$$\frac{\partial N_{xy}}{\partial x} + \frac{\partial N_y}{\partial y} + R - \sum_{i=1}^{N} R_i \delta(x - x_i)\delta(y - y_i) = 0 \tag{1b}$$

$$\begin{aligned}&\frac{\partial^2 M_x}{\partial x^2} + 2\frac{\partial^2 M_{xy}}{\partial x \partial y} + \frac{\partial^2 M_y}{\partial y^2} + N_x \frac{\partial^2 w}{\partial x^2} + 2N_{xy}\frac{\partial^2 w}{\partial x \partial y} \\ &\quad + N_y \frac{\partial^2 w}{\partial y^2} + q - \left[\sum_{i=1}^{N} q_i \delta(x - x_i)\delta(y - y_i)\right] + \frac{\partial V}{\partial x}\left(\frac{t}{2}\right) \\ &\quad - \left[\sum_{i=1}^{N} V_i \delta'(x - x_i)\delta(y - y_i)\right]\left(\frac{t}{2}\right) + \frac{\partial R}{\partial y}\left(\frac{t}{2}\right) \\ &\quad - \left[\sum_{i=1}^{N} R_i \delta(x - x_i)\delta'(y - y_i)\right]\left(\frac{t}{2}\right) = 0\end{aligned} \tag{1c}$$

where (N_x, N_y, N_{xy}) and (M_x, M_y, M_{xy}) are stress resultants and stress couples, respectively; $\delta(x - x_i)$ and $\delta(y - y_i)$ are the Dirac delta functions; and x and y are in-plane coordinates.

For homogeneous orthotropic face plates, $B_{ij} = A_{16} = A_{26} = D_{16} = D_{26} = 0$, the constitutive equation is

$$\begin{Bmatrix} N_x \\ N_y \\ N_{xy} \\ \hline M_x \\ M_y \\ M_{xy} \end{Bmatrix} = \left(\begin{array}{ccc|ccc} A_{11} & A_{12} & 0 & & & \\ A_{12} & A_{22} & 0 & & 0 & \\ 0 & 0 & A_{66} & & & \\ \hline & & & D_{11} & D_{12} & 0 \\ & 0 & & D_{12} & D_{22} & 0 \\ & & & 0 & 0 & D_{66} \end{array}\right) \begin{Bmatrix} \epsilon_x \\ \epsilon_y \\ \epsilon_{xy} \\ \hline \kappa_x \\ \kappa_y \\ \kappa_{xy} \end{Bmatrix} \tag{2}$$

in which

$$\begin{aligned} &\epsilon_x = \frac{\partial u}{\partial x} \qquad \epsilon_y = \frac{\partial v}{\partial y} \qquad \epsilon_{xy} = \frac{\partial u}{\partial y} + \frac{\partial v}{\partial x} \\ &\kappa_x = -\frac{\partial^2 w}{\partial x^2} \qquad \kappa_y = -\frac{\partial^2 w}{\partial y^2} \qquad \kappa_{xy} = -2\frac{\partial^2 w}{\partial x \partial y} \end{aligned} \tag{3}$$

where u, v, and w are in-plane displacements of the middle plane and transverse displacement of the face plate, respectively; $(\epsilon_x, \epsilon_y, \epsilon_{xy})$ are in-plane strain components; and $(\kappa_x, \kappa_y, \kappa_{xy})$ are curvature components. By substituting Eqs. (2) and (3) into Eqs. (1a–1c), we obtain

$$A_{11}\frac{\partial^2 u}{\partial x^2} + A_{12}\frac{\partial^2 v}{\partial x \partial y} + A_{66}\left(\frac{\partial^2 u}{\partial y^2} + \frac{\partial^2 v}{\partial x \partial y}\right) + V - \sum_{i=1}^{N} V_i \delta(x - x_i)\delta(y - y_i) = 0 \tag{4a}$$

$$A_{66}\left(\frac{\partial^2 u}{\partial x \partial y} + \frac{\partial^2 v}{\partial x^2}\right) + A_{12}\frac{\partial^2 u}{\partial x \partial y} + A_{22}\frac{\partial^2 v}{\partial y^2} + R - \sum_{i=1}^{N} R_i \delta(x - x_i)\delta(y - y_i) = 0 \tag{4b}$$

$$D_{11}\frac{\partial^4 w}{\partial x^4} + 2(D_{12}+2D_{66})\frac{\partial^4 w}{\partial x^2 \partial y^2} + D_{22}\frac{\partial^4 w}{\partial y^4} - N_x\frac{\partial^2 w}{\partial x^2}$$

$$- 2N_{xy}\frac{\partial^2 w}{\partial x \partial y} - N_y\frac{\partial^2 w}{\partial y^2} - q + \left[\sum_{i=1}^{N} q_i \delta(x-x_i)\delta(y-y_i)\right]$$

$$- \frac{\partial V}{\partial x}\left(\frac{t}{2}\right) + \left[\sum_{i=1}^{N} V_i \delta'(x-x_i)\delta(y-y_i)\right]\left(\frac{t}{2}\right)$$

$$- \frac{\partial R}{\partial y}\left(\frac{t}{2}\right) + \left[\sum_{i=1}^{N} R_i \delta(x-x_i)\delta'(y-y_i)\right]\left(\frac{t}{2}\right) = 0 \quad (4c)$$

We are only interested in the critical buckling loads of the face plate under compressive loadings P_x and/or P_y in the x and y directions, respectively, in the present study; i.e.,

$$N_{xy} = 0 \qquad N_x = -P_x \qquad N_y = -P_y \quad (5)$$

For the core of the sandwich plates, the following load–deformation relations based on the commonly used simple model are used:

$$q = q(x, y) = -k_f \cdot w \quad (6)$$

with

$$k_f = \left(\frac{E_c \cdot A_{\text{eff}}}{c}\right)$$

$$V = V(x, y) = G_{xz}\gamma_{xz} \quad (7a)$$

$$R = R(x, y) = G_{xz}\gamma_{yz} \quad (7b)$$

with

$$\gamma_{xz} = \frac{[u + (t/2)(\partial w/\partial x)]}{(c/2)} \qquad \gamma_{yz} = \frac{[v + (t/2)(\partial w/\partial y)]}{(c/2)}$$

For the sake of convenience, we define two parameters $s_{fx} = G_{xz}/c$ and $s_{fy} = G_{xz}/c$. Thus, Eqs. (7a) and (7b) can be rewritten as follows:

$$V = V(x, y) = s_{fx}\left[2u + t\left(\frac{\partial w}{\partial x}\right)\right] \quad (8a)$$

$$R = R(x, y) = s_{fy}\left[2v + t\left(\frac{\partial w}{\partial y}\right)\right] \quad (8b)$$

By substituting Eqs. (5), (6), (8a), and (8b) into Eqs. (4a–4c), we may rewrite the governing equations as follows:

$$A_{11}\frac{\partial^2 u}{\partial x^2} + A_{12}\frac{\partial^2 v}{\partial x \partial y} + A_{66}\left(\frac{\partial^2 u}{\partial y^2} + \frac{\partial^2 v}{\partial x \partial y}\right) + 2s_{fx}u$$

$$+ ts_{fx}\frac{\partial w}{\partial x} - \sum_{i=1}^{N} V_i \delta(x-x_i)\delta(y-y_i) = 0 \quad (9a)$$

$$A_{66}\left(\frac{\partial^2 u}{\partial x \partial y} + \frac{\partial^2 v}{\partial x^2}\right) + A_{12}\frac{\partial^2 u}{\partial x \partial y} + A_{22}\frac{\partial^2 v}{\partial y^2} + 2s_{fy}v$$

$$+ ts_{fy}\frac{\partial w}{\partial y} - \sum_{i=1}^{N} R_i \delta(x-x_i)\delta(y-y_i) = 0 \quad (9b)$$

$$D_{11}\frac{\partial^4 w}{\partial x^4} + 2(D_{12}+2D_{66})\frac{\partial^4 w}{\partial x^2 \partial y^2} + D_{22}\frac{\partial^4 w}{\partial y^4} + P_x\frac{\partial^2 w}{\partial x^2}$$

$$+ P_y\frac{\partial^2 w}{\partial y^2} + k_f w + \left[\sum_{i=1}^{N} q_i \delta(x-x_i)\delta(y-y_i)\right] - ts_{fx}\frac{\partial u}{\partial x}$$

$$- \frac{t^2 s_{fx}}{2}\frac{\partial^2 w}{\partial x^2} + \left[\sum_{i=1}^{N} V_i \delta'(x-x_i)\delta(y-y_i)\right]\left(\frac{t}{2}\right) - ts_{fy}\frac{\partial v}{\partial y}$$

$$- \frac{t^2 s_{fy}}{2}\frac{\partial^2 w}{\partial y^2} + \left[\sum_{i=1}^{N} R_i \delta(x-x_i)\delta'(y-y_i)\right]\left(\frac{t}{2}\right) = 0 \quad (9c)$$

Analytical Solution

For an a by b rectangular plate with all hinged edges, which are free to move in the in-plane normal direction, the boundary conditions are at $x = 0, a$,

$$w = 0, \qquad M_x = -D_{11}\frac{\partial^2 w}{\partial x^2} - D_{12}\frac{\partial^2 w}{\partial y^2} = 0 \quad (10a)$$

$$v = 0, \qquad N_x = A_{11}\frac{\partial u}{\partial x} + A_{12}\frac{\partial v}{\partial y} = 0 \quad (10b)$$

at $y = 0, b$,

$$w = 0, \qquad M_y = -D_{12}\frac{\partial^2 w}{\partial x^2} - D_{22}\frac{\partial^2 w}{\partial y^2} = 0 \quad (10c)$$

$$u = 0, \qquad N_y = A_{12}\frac{\partial u}{\partial x} + A_{22}\frac{\partial v}{\partial y} = 0 \quad (10d)$$

The displacements satisfying the preceding boundary conditions are represented by the following double Fourier series:

$$u = \sum_{m=0}^{\infty}\sum_{n=1}^{\infty} u_{mn}\cos\alpha_m x \sin\beta_n y \quad (11a)$$

$$v = \sum_{m=1}^{\infty}\sum_{n=0}^{\infty} v_{mn}\sin\alpha_m x \cos\beta_n y \quad (11b)$$

$$w = \sum_{m=1}^{\infty}\sum_{n=1}^{\infty} w_{mn}\sin\alpha_m x \sin\beta_n y \quad (11c)$$

in which $\alpha_m = m\pi/a$, and $\beta_n = n\pi/b$.

We also expand the fictitious loadings to Fourier series,

$$\sum_{i=1}^{N} V_i \delta(x-x_i)\delta(y-y_i) = \sum_{m=0}^{\infty}\sum_{n=1}^{\infty}\left(\sum_{i=1}^{N} V_i F_{mni}^{V}\right)\cos\alpha_m x \sin\beta_n y \quad (12a)$$

$$\sum_{i=1}^{N} R_i \delta(x-x_i)\delta(y-y_i) = \sum_{m=1}^{\infty}\sum_{n=0}^{\infty}\left(\sum_{i=1}^{N} R_i F_{mni}^{R}\right)\sin\alpha_m x \cos\beta_n y \quad (12b)$$

$$\sum_{i=1}^{N} q_i \delta(x-x_i)\delta(y-y_i) = \sum_{m=1}^{\infty}\sum_{n=1}^{\infty}\left(\sum_{i=1}^{N} q_i F_{mni}^{q}\right)\sin\alpha_m x \sin\beta_n y \quad (12c)$$

$$\sum_{i=1}^{N} V_i \delta'(x-x_i)\delta(y-y_i) = \sum_{m=1}^{\infty}\sum_{n=1}^{\infty}\left[\sum_{i=1}^{N} V_i(-\alpha_m) F_{mni}^{V}\right]\sin\alpha_m x \sin\beta_n y \quad (12d)$$

$$\sum_{i=1}^{N} R_i \delta(x-x_i)\delta'(y-y_i) = \sum_{m=1}^{\infty}\sum_{n=1}^{\infty}\left[\sum_{i=1}^{N} R_i(-\beta_n) F_{mni}^{R}\right]\sin\alpha_m x \sin\beta_n y \quad (12e)$$

where

$$F_{0ni}^{V} = (2/ab)\sin\beta_n y_i \qquad F_{m0i}^{R} = (2/ab)\sin\alpha_m x_i$$

$$F_{mni}^{V} = (4/ab)\cos\alpha_m x_i \sin\beta_n y_i$$

$$F_{mni}^{R} = (4/ab)\sin\alpha_m x_i \cos\beta_n y_i$$

$$F_{mni}^{q} = (4/ab)\sin\alpha_m x_i \sin\beta_n y_i$$

By substituting Eqs. (11a–11c) and (12a–12e) into Eqs. (9a–9c), we obtain

$$a_{11}\bar{u}_{mn} + a_{12}\bar{v}_{mn} + a_{13}\bar{w}_{mn} = \sum_{k=1}^{N} \bar{V}_i A_{mni} \tag{13a}$$

$$a_{21}\bar{u}_{mn} + a_{22}\bar{v}_{mn} + a_{23}\bar{w}_{mn} = \sum_{k=1}^{N} \bar{R}_i B_{mni} \tag{13b}$$

$$a_{31}\bar{u}_{mn} + a_{32}\bar{v}_{mn} + a_{33}\bar{w}_{mn} = -\sum_{k=1}^{N} (\bar{q}_i C_{mni} + \bar{V}_i D_{mni} + \bar{R}_i E_{mni}) \tag{13c}$$

where

$$a_{11} = -m^2\pi^2\bar{A}_{11} - n^2\pi^2\bar{R}^2\bar{A}_{66} + 2\bar{R}^2\bar{s}_{fx}$$

$$a_{12} = -mn\pi^2\bar{R}\bar{A}_{12} - mn\pi^2\bar{R}\bar{A}_{66} \qquad a_{13} = m\pi\bar{t}\bar{R}\bar{s}_{fx}$$

$$a_{21} = -mn\pi^2\bar{R}\bar{A}_{66} - mn\pi^2\bar{R}\bar{A}_{12}$$

$$a_{22} = -m^2\pi^2\bar{A}_{66} - n^2\pi^2\bar{R}^2\bar{A}_{22} + 2\bar{R}^2\bar{s}_{fy} \qquad a_{23} = n\pi\bar{t}\bar{R}^2\bar{s}_{fy}$$

$$a_{31} = m\pi\bar{t}\bar{R}\bar{s}_{fx} \qquad a_{32} = n\pi\bar{t}\bar{R}^2\bar{s}_{fy}$$

$$a_{33} = \{(D_{11}/D_{22}) + (1/\bar{R}^2)m^4\pi^2 + 2(D_{12}/D_{22}) + 2(D_{66}/D_{22})m^2n^2\pi^4 + n^4\pi^4\bar{R}^2 + m^2\pi^2\bar{P}_x + n^2\pi^2\bar{R}^2\bar{P}_y + \bar{K}\bar{R}^2 + \tfrac{1}{2}m^2\pi^2\bar{t}^2\bar{s}_{fx} + \tfrac{1}{2}n^2\pi^2\bar{t}^2\bar{R}^2\bar{s}_{fy}\}$$

$$A_{mni} = 4\sum_{i=1}^{N} \bar{V}_i \bar{R}\cos\alpha_m x_i \sin\beta_n y_i$$

$$B_{mni} = 4\sum_{i=1}^{N} \bar{R}_i \bar{R}\sin\alpha_m x_i \cos\beta_n y_i$$

$$C_{mni} = 4\sum_{i=1}^{N} \bar{q}_i \bar{R}\sin\alpha_m x_i \sin\beta_n y_i$$

$$D_{mni} = -2\sum_{i=1}^{N} \bar{V}_i \bar{t} m\pi \cos\alpha_m x_i \sin\beta_n y_i$$

$$E_{mni} = -2\sum_{i=1}^{N} \bar{R}_i \bar{t}\bar{R} n\pi \sin\alpha_m x_i \cos\beta_n y_i$$

with

$$\bar{A}_{11} = \frac{A_{11}b^2}{D_{22}} \qquad \bar{A}_{66} = \frac{A_{66}b^2}{D_{22}}$$

$$\bar{A}_{12} = \frac{A_{12}b^2}{D_{22}} \qquad \bar{A}_{22} = \frac{A_{22}b^2}{D_{22}}$$

$$\bar{s}_{fx} = \frac{s_{fx}b^4}{D_{22}} \qquad \bar{s}_{fy} = \frac{s_{fy}b^4}{D_{22}}$$

$$\bar{u}_{mn} = u_{mn}/b \qquad \bar{v}_{mn} = v_{mn}/b$$

$$\bar{w}_{mn} = w_{mn}/b \qquad \bar{K} = k_f b^4/D_{22}$$

$$\bar{P}_x = P_x b^2/D_{22} \qquad \bar{P}_y = P_y b^2/D_{22}$$

$$\bar{V}_i = V_i b/D_{22} \qquad \bar{R}_i = R_i b/D_{22}$$

$$\bar{q}_i = q_i b/D_{22} \qquad \bar{R} = a/b \qquad \bar{t} = t/b$$

By employing Cramer's rule to solve the algebraic equations in terms of $\bar{u}_{mn}$, $\bar{v}_{mn}$, and $\bar{w}_{mn}$, we obtain

$$\bar{u}_{mn} = \sum_{i=1}^{N} \bar{A}_{mni}\bar{q}_i + \sum_{i=0}^{N} \bar{B}_{mni}\bar{V}_i + \sum_{i=1}^{N} \bar{C}_{mni}\bar{R}_i \tag{14a}$$

$$\bar{v}_{mn} = \sum_{i=1}^{N} \bar{D}_{mni}\bar{q}_i + \sum_{i=1}^{N} \bar{E}_{mni}\bar{V}_i + \sum_{i=1}^{N} \bar{F}_{mni}\bar{R}_i \tag{14b}$$

$$\bar{w}_{mn} = \sum_{i=1}^{N} \bar{G}_{mni}\bar{q}_i + \sum_{i=1}^{N} \bar{H}_{mni}\bar{V}_i + \sum_{i=1}^{N} \bar{I}_{mni}\bar{R}_i \tag{14c}$$

in which

$$\bar{A}_{mni} = (1/\Delta)(a_{22}a_{13} - a_{12}a_{23})C_{mni}$$

$$\bar{B}_{mni} = (1/\Delta)[(a_{22}a_{33} - a_{32}a_{23})A_{mni} - (a_{12}a_{23} - a_{22}a_{13})D_{mni}]$$

$$\bar{C}_{mni} = (1/\Delta)[(a_{32}a_{13} - a_{12}a_{33})B_{mni} - (a_{12}a_{23} - a_{22}a_{13})E_{mni}]$$

$$\bar{D}_{mni} = (1/\Delta)(a_{11}a_{23} - a_{21}a_{13})C_{mni}$$

$$\bar{E}_{mni} = (1/\Delta)[(a_{31}a_{23} - a_{21}a_{33})A_{mni} - (a_{21}a_{13} - a_{11}a_{23})D_{mni}]$$

$$\bar{F}_{mni} = (1/\Delta)[(a_{11}a_{33} - a_{31}a_{13})B_{mni} - (a_{21}a_{13} - a_{11}a_{23})E_{mni}]$$

$$\bar{G}_{mni} = (1/\Delta)(-a_{11}a_{22} + a_{21}a_{12})C_{mni}$$

$$\bar{H}_{mni} = (1/\Delta)[(a_{21}a_{32} - a_{31}a_{22})A_{mni} - (a_{11}a_{22} - a_{21}a_{12})D_{mni}]$$

$$\bar{I}_{mni} = (1/\Delta)[(a_{31}a_{12} - a_{11}a_{32})B_{mni} - (a_{11}a_{22} - a_{21}a_{12})E_{mni}]$$

with

$$\Delta = \begin{vmatrix} a_{11} & a_{12} & a_{13} \\ a_{21} & a_{22} & a_{23} \\ a_{31} & a_{32} & a_{33} \end{vmatrix}$$

Now, we have general solutions for u, v, and w from which we obtain $q(x, y)$, $V(x, y)$, and $R(x, y)$ from Eqs. (6), (7a), and (7b), respectively. To require net interfacial stresses in the delaminated region to vanish, the following conditions must be satisfied at every subdivision:

$$\iint_{\Delta A_j} q(x, y)\,dx\,dy = q_j \tag{15a}$$

$$\iint_{\Delta A_j} V(x, y)\,dx\,dy = V_j \tag{15b}$$

$$\iint_{\Delta A_j} R(x, y)\,dx\,dy = R_j \tag{15c}$$

in which ΔA_j represents the area of the jth subdivision in the debonded region; the subscript j ranging from 1 to N is the number of subdivisions in the debonded region that are considered to be rectangular or circular shapes, as shown in Figs. 2a–2d. The rectangular delaminated region is subdivided into rectangular subdivisions where fictitious forces are applied. However, for circular regions, radial and circumferential lines are used to subdivide the delaminated regions. Equations (15a–15c) may be approximated for small enough ΔA_j by

$$\text{at} \quad x = x_j, \qquad y = y_j \qquad q(x_j, y_j)\Delta A_j = q_j \tag{16a}$$

$$\text{at} \quad x = x_j, \qquad y = y_j \qquad V(x_j, y_j)\Delta A_j = V_j \tag{16b}$$

$$\text{at} \quad x = x_j, \qquad y = y_j \qquad R(x_j, y_j)\Delta A_j = R_j \tag{16c}$$

Substitutions of Eqs. (6), (8a), (8b), and (11a–11c) in conjunction with Eqs. (14a–14c) into Eqs. (16a–16c) yield a system of $3N$ homogenuous algebraic equations that could be written in a matrix form as follows:

$$[A]\{X\} = 0 \tag{17}$$

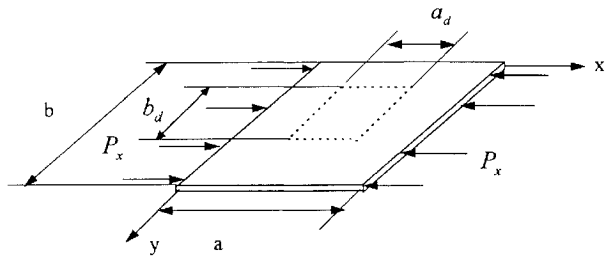

a) Central rectangular delamination

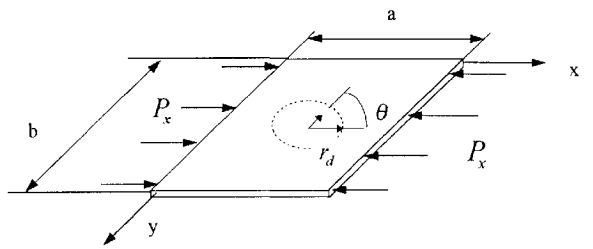

b) Central circular delamination

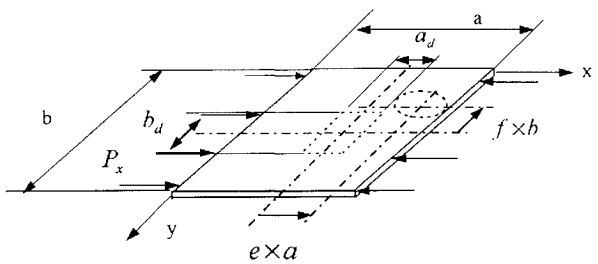

c) Multiple delaminations

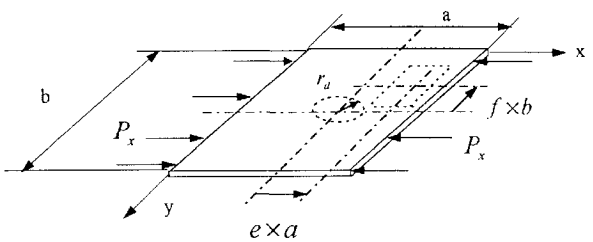

d) Multiple delaminations

Fig. 2 Simply supported square sandwich plate with different types of delamination subjected to uniform uniaxial compression.

Here $[A]$ is a $3N \times 3N$ matrix containing buckling loads as parameters, and $\{X\} = [q_i \;\; V_i \;\; R_i]^T$ for i ranging from 1 to N is a $3N \times 1$ column matrix. Equation (17) may be expressed as

$$\left(\begin{array}{c|c|c} A^*_{ji} & B^*_{ji} & C^*_{ji} \\ \hline D^*_{ji} & E^*_{ji} & F^*_{ji} \\ \hline G^*_{ji} & H^*_{ji} & I^*_{ji} \end{array}\right) \left\{\begin{array}{c} \bar{q}_i \\ \hline \bar{V}_i \\ \hline \bar{R}_i \end{array}\right\} = 0 \tag{18}$$

where

$$A^*_{ji} = \sum_{m=0}^{\infty}\sum_{n=1}^{\infty}(2\Phi_x \bar{A}_{mni} + \Psi_x m\pi \bar{G}_{mni}) \cos\alpha_m x_j \sin\beta_n y_j$$

$$B^*_{ji} = \sum_{m=0}^{\infty}\sum_{n=1}^{\infty}(2\Phi_x \bar{B}_{mni} + \Psi_x m\pi \bar{H}_{mni}) \cos\alpha_m x_j \sin\beta_n y_j - \delta_{ij}$$

$$C^*_{ji} = \sum_{m=0}^{\infty}\sum_{n=1}^{\infty}(2\Phi_x \bar{C}_{mni} + \Psi_x m\pi \bar{I}_{mni}) \cos\alpha_m x_j \sin\beta_n y_j$$

$$D^*_{ji} = \sum_{m=1}^{\infty}\sum_{n=0}^{\infty}(2\Phi_y \bar{D}_{mni} + \Psi_y m\pi \bar{G}_{mni}) \sin\alpha_m x_j \cos\beta_n y_j$$

$$E^*_{ji} = \sum_{m=1}^{\infty}\sum_{n=0}^{\infty}(2\Phi_y \bar{E}_{mni} + \Psi_y m\pi \bar{H}_{mni}) \sin\alpha_m x_j \cos\beta_n y_j$$

$$F^*_{ji} = \sum_{m=1}^{\infty}\sum_{n=0}^{\infty}(2\Phi_y \bar{F}_{mni} + \Psi_y m\pi \bar{I}_{mni}) \sin\alpha_m x_j \cos\beta_n y_j - \delta_{ij}$$

$$G^*_{ji} = \sum_{m=1}^{\infty}\sum_{n=1}^{\infty}\Phi_k \bar{G}_{mni} \sin\alpha_m x_j \sin\beta_n y_j + \delta_{ij}$$

$$H^*_{ji} = \sum_{m=1}^{\infty}\sum_{n=1}^{\infty}\Phi_k \bar{H}_{mni} \sin\alpha_m x_j \sin\beta_n y_j$$

$$I^*_{ji} = \sum_{m=1}^{\infty}\sum_{n=1}^{\infty}\Phi_k \bar{I}_{mni} \sin\alpha_m x_j \sin\beta_n y_j$$

with

$$\Phi_x = \frac{ab\Delta A_j}{D_{22}} s_{fx} \qquad \Psi_x = \frac{bt\Delta A_j}{D_{22}} s_{fx} \qquad \Phi_y = \frac{ab\Delta A_j}{D_{22}} s_{fy}$$

$$\Psi_y = \frac{at\Delta A_j}{D_{22}} s_{fy} \qquad \Phi_k = \frac{ab\Delta A_j}{D_{22}} k_f$$

For buckling ploblems, the critical buckling load may be determined by requiring the determinant of the coefficient matrix of Eq. (18) to vanish.

Numerical Examples

Numerical results of several examples of the method and procedure schemes for treating rectangular and circular delamination shapes and for providing limited data to indicate effects of delamination size, location, and interaction of adjacent delaminations are obtained. Although the actual shape of delamination would generally be irregular, we established the schemes for handling rectangular and circular shapes with the only intention that they may potentially be used together to approximately describe actual irregular shaped delaminations in future studies. The data for the material properties are $E_1 = 40E_2$, $G_{12} = 0.5E_2$, and $\nu_{12} = 0.25$, where subscripts 1 and 2 denote directions parallel and transverse to the fiber directions, respectively; and the nondimensional parameters $\bar{k}_f$, $\bar{s}_x$, and $\bar{s}_y$ are used in all examples.

Rectangular Delaminations

We first consider a square sandwich plate with 0-deg laminated face sheets having a central square delamination subjected to a uniaxial compression P_x, as shown in Fig. 2a. Numerical results obtained by the present analysis for the uniaxial buckling load $P_x b^2/E_2 t^3$ are listed in Table 1. As expected, the buckling load decreases as the core stiffness ($\bar{k}_f$, $\bar{s}_x$, $\bar{s}_y$) decreases and as the delamination size (a_d and b_d) increases; the buckling load corresponding to very low stiffnesses of the core and very large delamination size should be close to that of the plates without foundation. A limited number of numerical results are presented in Table 1 for illustrating the anticipated facts and for validating the method of analysis and the computer program. All numerical data given in Table 1 are obtained by increasing the number of subdivisions until converged solutions are reached. Numerical results shown in the sixth and seventh rows of Table 1 indicate that when $\bar{s}_x (=\bar{s}_y)$ are reduced from 0.01 to 0.001, the buckling load parameter given in the last column is reduced but slightly from 55.619 to 54.140, which amounts to a less than 2.66% reduction. When comparing corresponding results in rows 1–3 with those in 4–6 rows, respectively, buckling loads are reduced by over 69% when $\bar{k}_f$ is reduced from 0.01 to 0.001 with $\bar{s}_x (=\bar{s}_y)$ increased from 0.001 to 0.01. These results indicate that the effect of $\bar{k}_f$ to the buckling load is more significant than $\bar{s}_x$ and $\bar{s}_y$. The remaining results listed from the seventh row down indicate that the buckling load parameter corresponding to low core stiffness $\bar{k}_f = \bar{s}_x = \bar{s}_y = 0.001$ becomes closer to the buckling load of 35.831 for the plate without foundation when the size of the delamination $a_d (=b_d)$ increases.[26] The present results for a_d/a with $a_d = b_d$ being 0.9 and 0.95 are 38.854 and 35.849, respectively. More comparisons for buckling loads of a sandwich plate with a

Table 1 Buckling loads for a square sandwich plate with one face sheet of composite 0-deg laminate having a central square delamination

a_d/a	b_d/b	$\bar{k}_f$	$\bar{s}_x$	$\bar{s}_y$	$P_x b^2/E_2 t^3$
0.01	0.01	0.01	0.001	0.001	183.61
0.05	0.05	0.01	0.001	0.001	183.00
0.10	0.10	0.01	0.001	0.001	182.23
0.01	0.01	0.001	0.01	0.01	56.454
0.05	0.05	0.001	0.01	0.01	56.262
0.10	0.10	0.001	0.01	0.01	55.619
0.1	0.1	0.001	0.001	0.001	54.140
0.2	0.2	0.001	0.001	0.001	52.225
0.3	0.3	0.001	0.001	0.001	49.136
0.4	0.4	0.001	0.001	0.001	45.299
0.5	0.5	0.001	0.001	0.001	41.829
0.6	0.6	0.001	0.001	0.001	39.294
0.7	0.7	0.001	0.001	0.001	37.447
0.8	0.8	0.001	0.001	0.001	36.226
0.9	0.9	0.001	0.001	0.001	35.854
0.95	0.95	0.001	0.001	0.001	35.849

Table 2 Uniaxial buckling loads for square sandwich plates with one face sheet of composite $(\pm\theta)_\infty$ laminate having a central square delamination

θ	$P_x b^2/E_2 t^3$, present[a]	$P_x b^2/E_2 t^3$, Ref. 25[b]
0	35.849	35.831
15	43.781	43.760
30	59.849	59.619
45	67.551	67.548
60	54.196	54.115
75	25.196	25.129
90	13.156	13.132

[a]Present analysis with $a_d/a = 0.95$ and $\bar{k}_f = \bar{s}_x = \bar{s}_y = 0.001$.
[b]Solution of simply supported square composite laminates (corresponding to $a_d/a = 1.0$).

large delamination size of $a_d/a = 0.95$ by $b_d/b = 0.95$ and very small core stiffnesses ($\bar{k}_f = \bar{s}_x = \bar{s}_y = 0.001$) from the present analysis to that of Ref. 25 for simply supported square composite laminate, with different fiber orientations, are given in Table 2. Results listed in Table 2 show that the values of the present analysis are all close to those of Ref. 25. The confirmation of anticipated facts and excellent agreements to existing exact solutions show that the present analysis is effective and reliable. Inasmuch as the size of the delamination varying from as small as $0.01a \times 0.01a$ to as large as $0.95a \times 0.95a$ are involved, this indicates that the method has no limitation on the size of delaminations.

To provide some indication of the effect of the core stiffnesses, a central $0.1a \times 0.1a$ delamination in a square plate having 0-deg face sheets as shown in Fig. 2a is considered. The uniaxial buckling load varies with core stiffnesses. The nondimensional uniaxial buckling loads with varying transverse stiffnesses are shown in Fig. 3; the buckling load varies nearly as linear functions of core stiffnesses. The variation is rapid for $\bar{k}_f$ ranging from 0.01 to 0.06 with small core shear stiffnesses $\bar{s}_x = \bar{s}_y = 0.001$ and is slower for $\bar{k}_f$ ranging from 0.06 to 0.1. For $\bar{k}_f = 0.001$, the buckling load parameter varies gradually as shear stiffnesses of $\bar{s}_x (= \bar{s}_y)$ vary from 0.01 to 0.04 and rapidly from 0.04 to 0.1. Note from curve a that the buckling load increases by as much as about 130% when the normal stiffness of core $\bar{k}_f$ increases from 0.01 to 0.06, whereas it exhibits only about an 18% increase when the normal stiffness increases from 0.06 to 0.1. From curve b, the buckling load increases as much as about 113% when shear stiffnesses increase from 0.04 to 0.1, whereas it exhibits only about 15% increase of buckling load when the shear stiffnesses increase from 0.01 to 0.04. Results shown in Fig. 3 reflect that the effect of normal stiffness $\bar{k}_f$ on buckling load is more significant than the effect of shear stiffnesses $\bar{s}_x$ and $\bar{s}_y$.

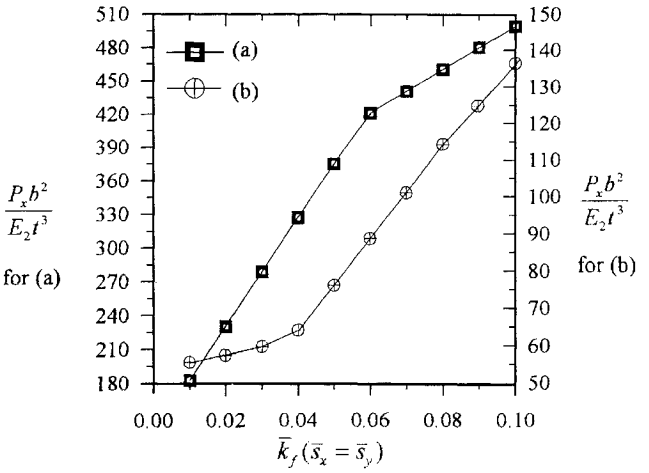

Fig. 3 Effect of transverse stiffnesses of the core on uniaxial buckling load ($a_d/a = b_d/b = 0.1$): a) various $\bar{k}_f$ with $\bar{s}_x = \bar{s}_y = 0.001$ and b) various $\bar{s}_x = \bar{s}_y$ with $\bar{k}_f = 0.001$.

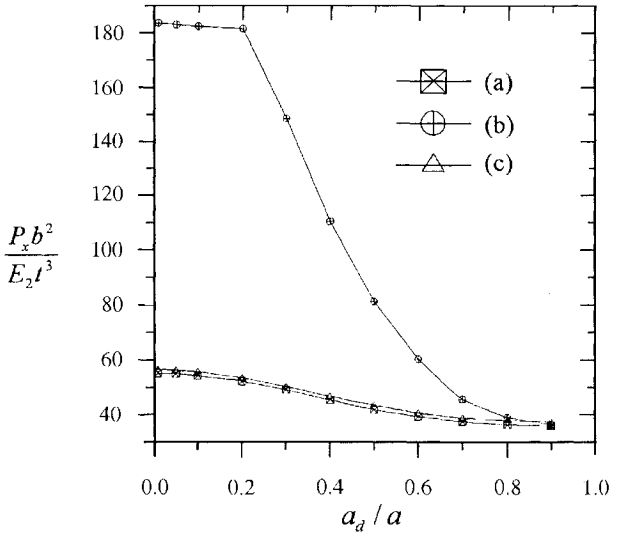

Fig. 4 Effect of delamination size on uniaxial buckling load: a) $\bar{k}_f = 0.001$ and $\bar{s}_x = \bar{s}_y = 0.001$, b) $\bar{k}_f = 0.01$ and $\bar{s}_x = \bar{s}_y = 0.001$, and c) $\bar{k}_f = 0.001$ and $\bar{s}_x = \bar{s}_y = 0.01$.

To investigate the effect of delamination size on the buckling load, we again consider a square delaminated sandwich plate with 0-deg composite face sheets under uniaxial compressive load of P_x on a face sheet. With $a_d/a = b_d/b$, variations of the buckling load parameter with respect to the delamination size characterized by a_d/a from three different combinations of core stiffnesses are shown in Fig. 4. As expected, the buckling load decreases as the delamination size increases. Curves also show that the increase of buckling load as a result of the increase of $\bar{k}_f$ is substantially higher than the increase of $\bar{s}_x$ and $\bar{s}_y$ for delamination size a_d/a less than about 0.75, and the rate of reduction of the buckling load is much more rapid for plate with $\bar{k}_f = 0.01$ than that with $\bar{k}_f = 0.001$ when the delamination size a_d/a increases from about 0.2. These results indicate that the effect of delamination size on the buckling load depends more heavily on the normal stiffness than the shear stiffnesses of the core.

To explore the effect of the delamination location on the buckling load, we consider a square sandwich plate having a $0.1a \times 0.1b$ square delamination with its center location varying along $x = a/2$. The nondimensional uniaxial buckling load corresponding to various delamination locations and transverse normal stiffnesses with $\bar{s}_x = \bar{s}_y = 0.001$ are shown in Fig. 5. There is no significant effect of the delamination location on the buckling load probably because of the small delamination size, which is 1% of the total plate area.

Table 3 Buckling loads for a square sandwich plate with one face sheet of composite 0-deg laminate having a central circular delamination

r_d/a	$\bar{k}_f$	$\bar{s}_x$	$\bar{s}_y$	$P_x b^2/E_2 t^3$
0.01	0.01	0.001	0.001	183.47
0.05	0.01	0.001	0.001	182.29
0.10	0.01	0.001	0.001	181.55
0.01	0.001	0.01	0.01	56.440
0.05	0.001	0.01	0.01	55.777
0.10	0.001	0.01	0.01	53.462
0.10	0.001	0.001	0.001	52.352
0.20	0.001	0.001	0.001	46.855
0.30	0.001	0.001	0.001	40.368
0.40	0.001	0.001	0.001	36.884
0.45	0.001	0.001	0.001	35.984

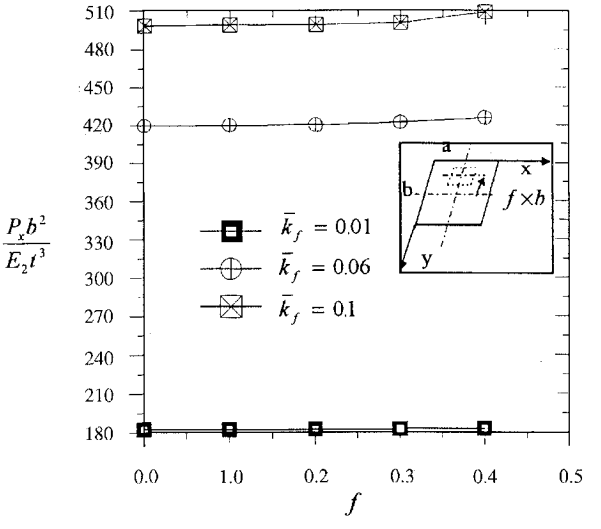

Fig. 5 Effect of delamination location on uniaxial buckling load (a_d/a = b_d/b = 0.1 and $\bar{s}_x = \bar{s}_y$ = 0.001).

Table 4 Buckling loads for a square sandwich plate with one face sheet of composite 0-deg laminate having two separated delaminations ($\bar{k}_f$ = 0.001 and $\bar{s}_x = \bar{s}_y$ = 0.001)

$e(f = 0.0)$	$P_x b^2/E_2 t^3$	$e = f$	$P_x b^2/E_2 t^3$
Case a: multiple delaminations shown in Fig. 2c			
0.25	166.48	0.25	167.41
0.30	170.00	0.30	172.81
0.35	174.71	0.35	179.55
Case b: multiple delaminations shown in Fig. 2d			
0.25	180.54	0.25	181.16
0.30	180.66	0.30	181.35
0.35	180.95	0.35	181.47

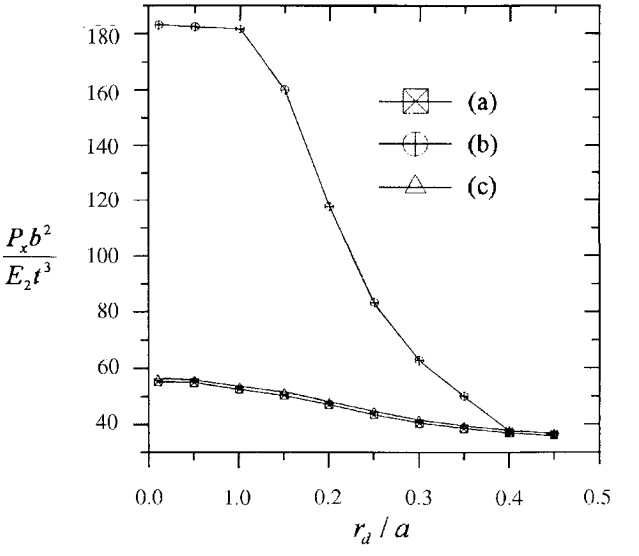

Fig. 6 Effect of delamination size on uniaxial buckling load: a) $\bar{k}_f$ = 0.001 and $\bar{s}_x = \bar{s}_y$ = 0.001, b) $\bar{k}_f$ = 0.01 and $\bar{s}_x = \bar{s}_y$ = 0.001, and c) $\bar{k}_f$ = 0.001 and $\bar{s}_x = \bar{s}_y$ = 0.01.

Circular Delaminations

We consider a square sandwich plate with composite 0-deg laminate face sheets having a central circular delamination of radius r_d as shown in Fig. 2b. The nondimensional uniaxial buckling loads for this plate with various delamination sizes and core stiffnesses are given in Table 3. All numerical results are consistent with those for rectangular delaminations to reflect the anticipated facts that the buckling load decreases as $\bar{k}_f$, $\bar{s}_x$, and $\bar{s}_y$ decrease and as the delamination size increases. Again, the buckling load of the plate with very small stiffnesses of the core ($\bar{k}_f = \bar{s}_x = \bar{s}_y = 0.001$) reduces to 35.984 for $r_d = 0.45$, which is very close to the value of 35.831 for the simply supported square composite 0-deg laminate given in Ref. 26. The scheme established for subdividing the circular delaminated region between radial and circumferential lines should give more accurate results than the use of rectangular subdivisions for the present class of problems. Seemingly, the present subdividing schemes may be extended to delamination shapes that have a combination of rectangles and circular sectors or to delaminated regions having curved boundaries.

To explore the effect of delamination size on the buckling load, we use the same square sandwich plate considered before but a circular delamination as shown in Fig. 2b. Buckling corresponding to various delamination sizes is shown in Fig. 6. Obviously, it displays results similar to those shown in Fig. 4 for the plate with a rectangular delamination.

Multiple Delaminations

To show the capability of the present analysis on a sandwich plate with multiple delaminations, we consider the case of a square sandwich plate with composite 0-deg laminated face sheets having two separated delaminations for which one is rectangular and the other one is circular. One delamination center is located at the center of the plate, and the center of the second delamination is located off the center of the plate. They are referred to as central and off-center delaminations, respectively. The location of the center of the off-center delamination is specified by e and f as shown in Figs. 2c and 2d. The size of the square delamination is considered to be $a_d = 0.2a$, and the radius of the circular delamination $r_d = 0.1a$ is used. Table 4 gives the nondimensional uniaxial buckling loads for $\bar{k}_f = 0.01$ and $\bar{s}_x = \bar{s}_y = 0.001$ corresponding to different locations of the off-center delamination. Case a in Table 4 associated with Fig. 2c concerns the sandwich plate containing a central square delamination. Results showing small decreases of the buckling load as the off-center delamination moves closer to the central delamination indicated a mild interaction of the two separated delaminations. The lowest value of 166.48 for the buckling load parameter given in the table for case a compared with 181.38 for a plate with a single central rectangular delamination amounts to a less than 9% reduction. Case b in Table 4 associated with Fig. 2d, concerning a sandwich plate that contains a central circular delamination and an off-center square delamination, exhibits the same phenomenon described in case a. The lowest buckling load for case b in Table 4 is 180.54, which represents a less than 0.56% reduction from 181.55 for a sandwich plate having a single central circular delamination.

Concluding Remarks

A two-dimensional model of a delaminated face sheet of sandwich plates, on the basis of the Kirchhoffean plate theory, has been proposed. The concept of the continuous analysis procedure presented in this study has shown its applicability for analyzing sandwich plates with single or multiple delaminations.

According to the results obtained in this study, we can make the following concluding remarks.

1) The method presented in the study is simple, straightforward, and effective.

2) Although the extent of the delamination affecting the critical buckling load of sandwich plates depends on the size, number, and location of delaminated regions and stiffnesses of the core, no general conclusive statements can be made as only limited results for only specific materials have been computed for illustrative purposes.

3) The effect of normal stiffness of the core $\bar{k}_f$ on buckling load is more significant than the effect of shear stiffnesses of the core $\bar{s}_x$ and $\bar{s}_y$.

4) The interaction effect of separated delaminations appears to be mild.

Acknowledgment

The study was partially supported by the National Science Council of the Republic of China under Grant NSC 84-2212-E005-009.

References

[1]Chai, H., Babcock, C. D., and Knauss, W. G., "One Dimensional Modeling of Failure in Laminated Plates by Delamination Buckling," *International Journal of Solids and Structures*, Vol. 17, No. 8, 1981, pp.1069–1083.

[2]Yin, W.-L., and Wang, J. T. S., "The Strain Energy Release Rate in the Growth of a One-Dimensional Delamination," *Journal of Applied Mechanics*, Vol. 51, Dec. 1984, pp. 939–941.

[3]Simitses, G. J., Sallam, S., and Yin, W. L., "Effect of Delamination of Axially Loaded Homogeneous Laminated Plates," *AIAA Journal*, Vol. 23, No. 9, 1985, pp. 1437–1444.

[4]Wang, S. S., Zahlan, N. M., and Suemasu, H., "Compressive Stability of Delaminated Random Short-Fiber Composites, Part I—Modeling and Methods of Analysis," *Journal of Composite Materials*, Vol. 19, No. 4, 1985, pp. 296–316.

[5]Yin, W. L., Sallam, S., and Simitses, G. J., "Ultimate Axial Load Capacity of a Delaminated Beam-Plate," *AIAA Journal*, Vol. 24, No. 1, 1986, pp. 123–128.

[6]Kardomateas, G. A., and Schmueser, D. W., "Buckling and Postbuckling of Delaminated Composites Under Compressive Loads Including Transverse Shear Effects," *AIAA Journal*, Vol. 26, No. 3, 1988, pp. 337–343.

[7]Anastasiadis, J. S., and Simitses, G. J., "Spring Simulated Delamination of Axially-Loaded Flat Laminates," *Composite Structures*, Vol. 17, 1991, pp. 67–85.

[8]Chen, H.-P., "Shear Deformation Theory for Compressive Delamination Buckling and Growth," *AIAA Journal*, Vol. 29, No. 5, 1991, pp. 813–819.

[9]Bottega, W. J., and Maewal, A., "Delamination Buckling and Growth in Laminates," *Journal of Applied Mechanics*, Vol. 50, March 1983, pp. 184–189.

[10]Chai, H., and Babcock, C. D., "Two-Dimensional Modeling of Compressive Failure in Delaminated Laminates," *Journal of Composite Materials*, Vol. 19, No. 1, 1985, pp. 67–98.

[11]Shivakumar, K. N., and Whitcomb, J. D., "Buckling of a Sublaminate in a Quasi-Isotropic Composite Laminate," *Journal of Composite Materials*, Vol. 19, No. 1, 1985, pp. 2–18.

[12]Kassapoglou, C., "Buckling, Post-Buckling and Failure of Elliptical Delaminations in Laminates under Compression," *Composite Structures*, Vol. 9, 1988, pp. 139–159.

[13]Yin, W. L., and Jane, K. C., "Refined Buckling and Postbuckling Analysis of Two-Dimensional Delamination—I. Analysis and Validation," *International Journal of Solids and Structures*, Vol. 29, No. 5, 1992, pp. 591–610.

[14]Yeh, M. K., and Tan, C. M., "Buckling of Elliptically Delaminated Composite Plates," *Journal of Composite Materials*, Vol. 28, No. 1, 1994, pp. 36–52.

[15]Rao, K. M., "Buckling Analysis of Anisotropic Sandwich Plates Faced with Fiber-Reinforced Plastics," *AIAA Journal*, Vol. 23, No. 8, 1985, pp. 1247–1253.

[16]Minguest, P., Dngundji, J., and Lagace, P. A., "Buckling and Failure of Sandwich Plates with Graphite-Epoxy Faces and Various Cores," *Journal of Aircraft*, Vol. 25, No. 4, 1988, pp. 372–379.

[17]Kim, C. G., and Hong, C. S., "Buckling of Unbalanced Anisotropic Sandwich Plates with Finite Bonding Stiffness," *AIAA Journal*, Vol. 26, No. 8, 1988, pp. 982–988.

[18]Kardomateas, G. A., "Effect of an Elastic Foundation on the Buckling and Postbuckling of Delaminated Composite Under Compressive Loads," *Journal of Applied Mechanics*, Vol. 55, March 1988, pp. 238–241.

[19]Somers, M., Weller, T., and Abramovich, H., "Influence of Predetermined Delaminations on Buckling and Postbuckling of Composite Sandwich Beams," *Composite Structures*, Vol. 17, 1991, pp. 295–329.

[20]Frostig, Y., "Behavior of Delaminated Beam with Transversely Flexible Core—High Order Theory," *Composite Structures*, Vol. 20, 1992, pp. 1–16.

[21]Hwu, C., and Hu, J. S., "Buckling and Postbuckling of Delaminated Composite Sandwich Beams," *AIAA Journal*, Vol. 30, No. 7, 1992, pp. 1901–1908.

[22]Wang, J. T. S., "Continuous Analysis of Layered Structures with Debonds," *Chinese Journal of Mechanics*, Vol. 9, No. 2, 1993, pp. 81–90.

[23]Cheng, S. H., Lin, C. C., and Wang, J. T. S., "Local Buckling of Delaminated Sandwich Beams Using Continuous Analysis," *International Journal of Solids and Structures* (to be published).

[24]Wang, J. T. S., and Huang, J. T., "Strain Energy Release Rate of Delaminated Composite Plates Using Continuous Analysis," *Journal of Composites Engineering*, Vol. 4, No. 7, 1994, pp. 731–744.

[25]Heath, W. G., "Sandwich Construction—Correlation and Extension of Existing Theory of Flat Panels Subjected to Lengthwise Compression, Part 1: The Strength of Flat Sandwich Panels," *Aircraft Engineering*, Vol. 32, 1960, pp. 186–191.

[26]Jones, R. M., Morgan, H. S., and Whitney, J. M., "Buckling and Vibration of Antisymmetrically Laminated Angle-Ply Rectangular Plates," *Journal of Applied Mechanics*, Vol. 40, Dec. 1973, pp. 1143, 1144.